

Position Sensorless Direct Torque Control of Brushless DC Motor Drive Using Four-Switch, Three Phase Inverter

S. M. Seyedi, A. Halvaei Niasar, H. Moghbelli

Abstract – Today, cost reduction is important matter in all of the systems. In brushless dc (BLDC) motor drives, cost reduction can be achieved by elimination of three Hall Effect position sensors and reducing the number of power switches. On the other hand, in order to reduce the torque ripple, direct torque control (DTC) method can directly control the inverter states. To utilize simultaneous both advantages, reduction cost and minimization torque ripple, we proposed a novel reduced-part position sensorless DTC technique for a four-switch, three-phase BLDC motor drive in the constant torque region. The performance of the proposed scheme is verified via some simulations. Copyright © 2012 Praise Worthy Prize S.r.l. - All rights reserved.

Keywords: Brushless DC Motor Drives, Direct Torque Control, Four-Switch Inverter, Sensorless Control, Cost Reduction

Nomenclature

T_{em}	Electromagnetic torque
T_{ea}, T_{eb}, T_{ec}	Developed torque of phase a and b
$e_{s\alpha}, e_{s\beta}$	Stationary reference frame back-emf voltages
$i_{s\alpha}, i_{s\beta}$	Stationary reference frame stator currents
k_{α}, k_{β}	Stationary reference frame back-EMF constants
p	Number of magnetic poles
θ_e	Rotor position
ω_e	Electrical speed of the rotor
v_{ao}, v_{bo}	Terminal voltages

I. Introduction

The permanent magnet brushless dc (BLDC) motors have several advantages such as high efficiency, high torque density, low maintenance and simplicity in their structure and control. Thus, this machine has been used extensively in industrial, automotive and household products [1], [2], [3]. Cost reduction of BLDC motor drive has had growing interest over these years.

Traditional BLDC motor is controlled via six-switch three-phase inverter (SSTPI) and requires three Hall Effect position sensors for true commutation of the currents. Cost reduction can be achieved by using four-switch three-phase inverter (FSTPI) and elimination of the position sensors [4], [5], [6], [7]. To minimize low-frequency torque ripple and torque response time as compared to conventional pulse width modulation (PWM) current controlled BLDC motor drives, direct torque control (DTC) scheme have been used [8], [9].

Recently, a few researches have been published to control of BLDC motor using FSTPI based on DTC method [10], [11]. Ozturk et al. have been proved that the stator flux controller can be removed and only torque controller is enough in DTC method for SSTPI, because the amplitude of the stator flux linkage can't easily be controlled due to the sharp changes and the curved shape of the flux vector between two consecutive commutation points in the stator flux linkage locus [9]. Then they have been proposed a DTC scheme for FSTPI BLDC motor drives similar to SSTPI including the actual pre-stored back electromotive force (back-EMF) constant versus electrical rotor position look-up table, but in this method the torque ripple was high [10]. In Ref. [11], unlike the methods discussed in [9], [10], at all sectors phase-a and phase-b torque were independently controlled by the hysteresis torque controllers, and so, the torque ripple was reduced.

Position sensorless control scheme for a FSTPI BLDC motor drive, was proposed in [10] based on the zero crossing point (ZCP) detection of phase back-EMF voltage using defined error functions. The commutation instants are 30 degrees after detected ZCPs of the error functions, therefore this method need phase shift.

In this paper, in order to employ advantages of the reduction cost and minimization torque ripple, a novel scheme is presented that the DTC method using FSTPI is utilized simultaneous with position sensorless scheme.

II. BLDC Motor Drive Using Four-Switch, Three Phase Inverter

For a surface-mounted BLDC motor and in the stationary reference frame electromagnetic torque should

be calculated as below [8], [9]:

$$T_{em} = \frac{3}{2} \frac{P}{2} \left[\frac{e_\alpha}{\omega_e} i_{s\alpha} + \frac{e_\beta}{\omega_e} i_{s\beta} \right] = \frac{3}{2} \frac{P}{2} [k_\alpha (\theta_e) i_{s\alpha} + k_\beta (\theta_e) i_{s\beta}] \quad (1)$$

To eliminate the low-frequency torque oscillations caused by the non-ideal trapezoidal shape of the actual back-EMF waveform of the BLDC motor, pre-stored back-EMF versus electrical rotor position look-up tables are designed and used in (1) to the torque estimation [10].

Ideal phase back-EMF, current and phase torque profile of the three-phase BLDC motor drive with four switch inverter in CCW direction is shown in Fig. 1. It illustrates that in two-phase conduction, only two of the three-phase torque generates constant torque during every 60 electrical degrees and the remaining phase torque becomes zero as shown in Table I.

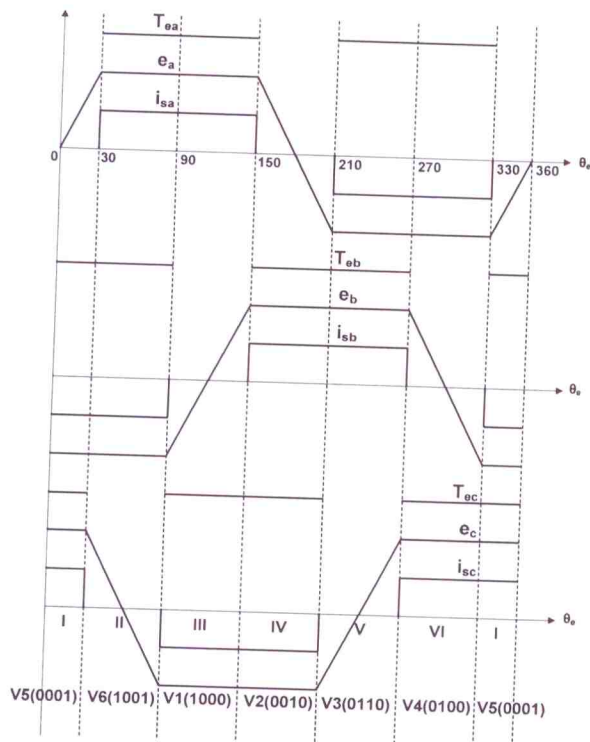


Fig. 1. Ideal phase back-EMF, current and phase torque profile of the three-phase BLDC motor drive with four switch inverter

TABLE I

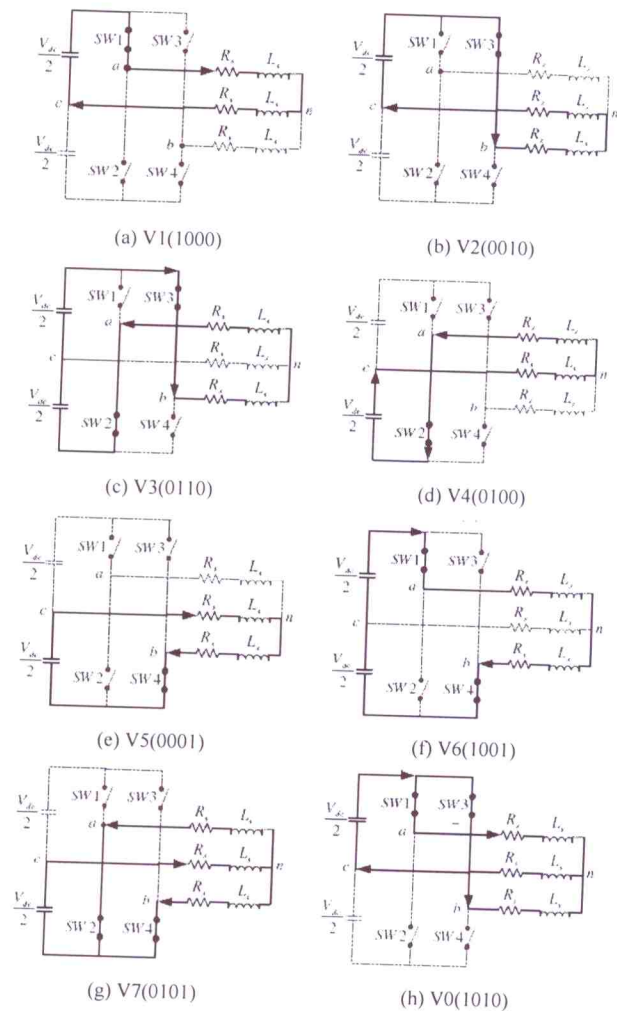
ELECTROMAGNETIC TORQUE EQUATION FOR THE OPERATING REGIONS

I : ($0^\circ < \theta < 30^\circ$ or $330^\circ < \theta < 360^\circ$)	$T_c = T_{eb} + T_{ec}$ & $T_{ea} = 0$
II : ($30^\circ < \theta < 90^\circ$)	$T_c = T_{ea} + T_{eb}$ & $T_{ec} = 0$
III : ($90^\circ < \theta < 150^\circ$)	$T_c = T_{ea} + T_{ec}$ & $T_{eb} = 0$
IV : ($150^\circ < \theta < 210^\circ$)	$T_c = T_{eb} + T_{ec}$ & $T_{ea} = 0$
V : ($210^\circ < \theta < 270^\circ$)	$T_c = T_{ea} + T_{eb}$ & $T_{ec} = 0$
VI : ($270^\circ < \theta < 330^\circ$)	$T_c = T_{ea} + T_{ec}$ & $T_{eb} = 0$

III. DTC of Four-Switch BLDC Motor Drive

When the DTC scheme for a BLDC motor is used, the stator flux linkage trajectory has sharp dips every 60 electrical degrees. This is due to the operation of the freewheeling diodes. Therefore, in the four-switch DTC of a BLDC motor drive with two-phase conduction scheme, the flux error in the voltage vector selection look-up table is always selected as zero and only the torque error is used depending on the error level of the actual torque from the reference torque [9].

Since the upper and lower switches in a phase leg may both be simultaneously off, in two-phase conduction mode, four digits are required for the four-switch inverter operation, one digit for each switch. also these eight useful voltage vectors are utilized as $V_0, 1, \dots, 6, 7$ (SW1, SW2, SW3, SW4) in Fig. 1, therefore the eight possible two-phase four-switch voltage vectors and current flow are depicted in Figs. 2.



Figs. 2. Four-switch voltage vector topology for two phase conduction DTC of BLDC motor drives

However, as shown in Figs. 2 two voltage vectors V3 and V6 create current distortion, because the back-EMF voltage of uncontrolled phase (phase-c) generates undesired current. Therefore, some ripples occur in phase's torque. As a result, undesired electromagnetic torque is inevitable. According to Fig. 1, when the rotor position is in the sector II and V, V6 and V3 are used respectively, so the torque of phase-a and phase-b should be independently controlled using the hysteresis torque controllers [10].

An Improved method is that at all sectors, phase-a and phase-b torque are independently controlled by the hysteresis torque controllers. This method causes the current and torque ripple to be reduced [11]. To obtain the six modes of operation in four-switch DTC of BLDC motor drive in ccw direction, a voltage vector selection look-up table is designed as shown in Table II.

TABLE II
TWO-PHASE FOUR-SWITCH VOLTAGE VECTOR SELECTION FOR DTC OF BLDC MOTOR DRIVE IN CCW DIRECTION

Phase-a,b Torque		Rotor angular position sector					
T_{ea}	T_{eb}	1	2	3	4	5	6
1	1	V5 (0001)	V6 (1001)	V1 (1000)	V2 (0010)	V3 (0110)	V4 (0100)
	-1	V2 (0010)	V0 (1010)	V1 (1000)	V5 (0001)	V7 (0101)	V4 (0100)
-1	1	V5 (0001)	V7 (0101)	V4 (0100)	V2 (0010)	V0 (1010)	V1 (1000)
	-1	V2 (0010)	V3 (0110)	V4 (0100)	V5 (0001)	V6 (1001)	V1 (1000)

The reference torque of both phases should be the half of the desired total reference torque as:

$$T_{ea_ref} = T_{eb_ref} = \frac{T_{ref}}{2} \quad (2)$$

The criteria utilized to implement the switching table for BLDC torque control can be explained as follows. Assume that the rotor flux vector is in sector I in CCW direction, i_{as} value is zero and i_{bs} value is negative.

Therefore $T_c = T_{eb} + T_{ec}$ and $T_{ea} = 0$, result $SW1 = SW2 = 0$. The torque of phase-c is uncontrollable due to its connect in to the midpoint of dc-link voltage, and so, the torque of phase-b is controllable, If T_{eb} is less than half of the reference torque, T_{eb} is "1" otherwise "-1". If $T_{eb} = 1$, to increase the torque of phase-b, $|i_b|$ should be increased, because i_b is negative. So, SW3 should be "0" and SW4 should be "1" and vice versa to decrease T_{eb} . In this sector T_{ea} is zero and so, it does not have role to determine the vector of this sector.

IV. Position Sensorless Control of Four-Switch BLDC Motor Drive

The main methods published in the literature about sensorless control of BLDC motor can be classified in five categories as: (1) Back-EMF sensing techniques (2)

Flux estimation method (3) stator inductance variations method (4) observers and classic control techniques and (5) using the special functions of motor variables [13].

The sensorless techniques that utilize the back-EMF voltage of the open-phase are more attractive due to their simplicity and ease of implementation, especially for low cost applications.

Commutation instants are 30° after zero crossing points of the phase back-EMF voltages, as shown in Fig. 1. On the other hand, back-EMF voltage of the stator is physical quantity that is hard to measure directly.

Therefore, detecting the motor terminal voltage is the simple way to find the ZCPs. In [10], three error functions in combination with two terminal voltages (of phases a and b) have been developed, in which they are synchronized with phase back-EMF voltages. These error functions (F_a, F_b, F_c) are defined as:

$$\begin{aligned} F_a(v_{ao}, v_{bo}) &= v_{ao} - 0.5v_{bo} \\ F_b(v_{ao}, v_{bo}) &= -v_{ao} + 2v_{bo} \\ F_c(v_{ao}, v_{bo}) &= -v_{ao} - v_{bo} \end{aligned} \quad (3)$$

The block diagram of the proposed position sensorless method has been shown in Fig. 3. Error functions are derived from the filtered terminal voltages v_{ao} and v_{bo} of two low-pass filters, which are used to eliminate high frequency noises for calculation of the average terminal voltages. Zero crossing detection of F_a, F_b and F_c generates three virtual hall position signals VH_a, VH_b and VH_c , respectively, which leads to the commutation points 30°. Therefore, to attain to the commutation points, depending on the motor speed, correct delay time should be used.

Determination of the error functions and detection of their ZCPs can be implemented via hardware or in software. However, creation a 30° delay is the lack of this method that results some position estimation error.

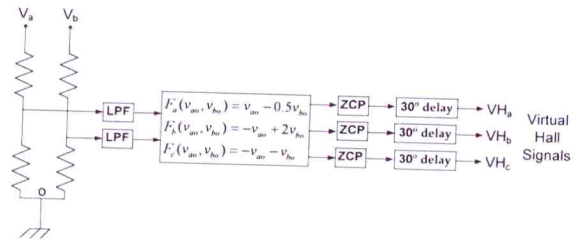


Fig. 3. Block diagram of the position sensorless based on the ZCP detection of phase back-EMF voltage

V. Simulation Results

The proposed block diagram of the position sensorless direct torque control of brushless DC motor using four-switch, three phase inverter in the constant torque region is represented in Fig. 4.

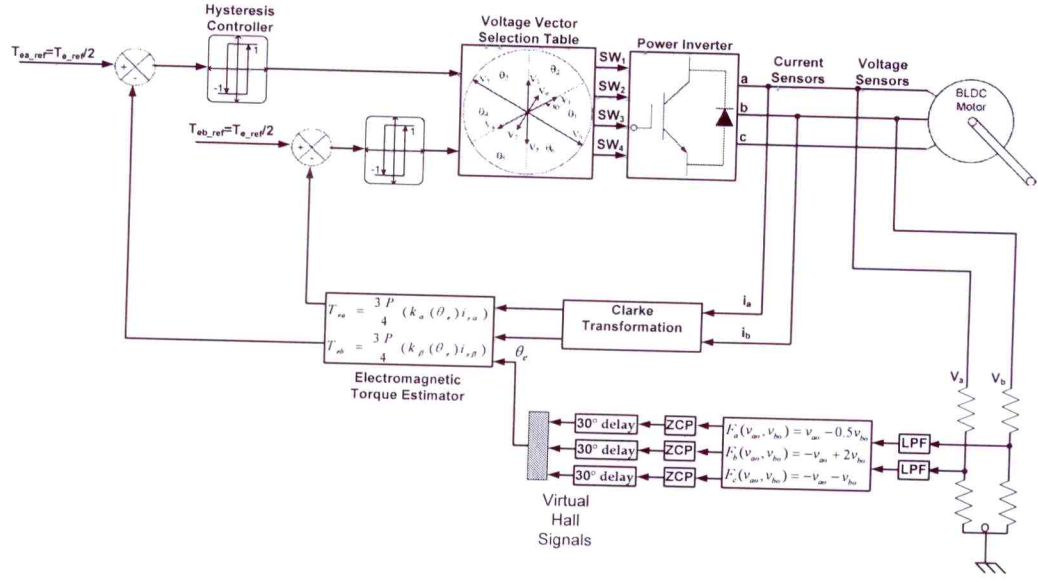


Fig. 4. Overall proposed block diagram of the position sensorless DTC of BLDC motor using FSTPI

The validity of the proposed technique is proved via some simulations in MATLAB/Simulink. Simulation results are obtained for 120° conduction angle BLDC motor with given parameters in Table III.

The actual values of $\alpha\beta$ -axes back-EMF constants k_{α} and k_{β} versus electrical rotor position θ_e are obtained as given below:

At first, phase back-EMFs versus time are obtained using MATLAB/Simulink at a reasonable fixed speed. Also, phase- a back-EMF voltage can be expressed as $E_a = k_a(\theta_e)\omega_e$ so, $k_a(\theta_e) = E_a/\omega_e = Et/(2\pi)$ where t is the total time in one electrical cycle. Therefore, phase- a back-EMF constant versus electrical rotor position $k_a(\theta_e)$ can be obtained. Similarly, the same method can be applied for $k_b(\theta_e)$. Finally, using Clarke transformation for phase back-EMF constants (abc to $\alpha\beta$), α - and β -axes back-EMF constants versus electrical rotor position are derived. The simulation results of the DTC method for FSTPI BLDC drive with position sensor has been shown in Fig. 5.

Then the simulation results of the proposed method by using sensorless method based on back-EMF voltages has been shown in Fig. 6. As the Figs. 5 and 6 have been shown, in both control methods ($\omega_{ref} = 100$ rpm), the torque and current ripple is same, therefore the proposed method decrease overall cost of BLDC drives without increasing torque and current ripple.

TABLE III
PARAMETERS OF BLDC MOTOR

Parameter	Symbol	Value
Phase Resistance	R	0.64[Ω]
Phase Self Inductance	L	1.0[mH]
Mutual Inductance	M	0.25[mH]
Rotor Pole Numbers	P	8[pole]
Rotor moment of Inertia	J	5e-4[kg.m ²]
Back-EMF Constant	K _e	0.0667[V/rpm]
DC Link Voltage	V _{dc}	60[V]
Rated Speed	ω_n	100[rpm]

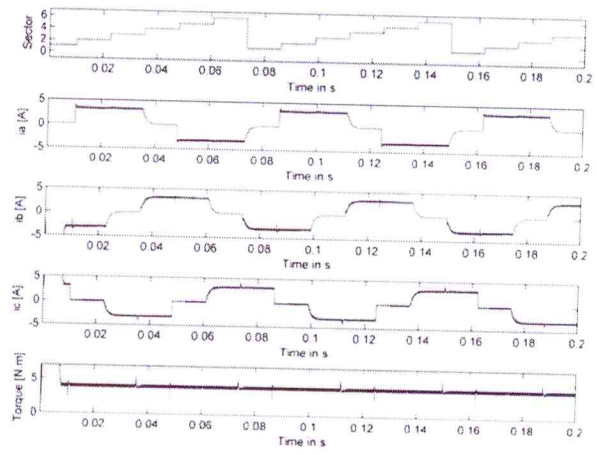


Fig. 5. Currents and generated torque in DTC for FSTPI BLDC with position sensor

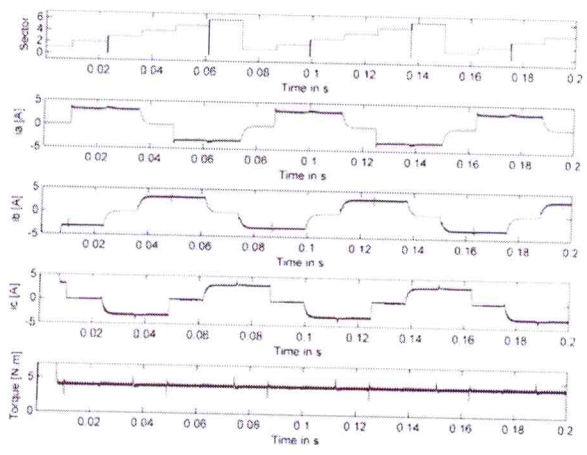


Fig. 6. Phase currents and generated torque in proposed position sensorless DTC for FSTPI BLDC

The simulation results of the proposed method with $\omega_{ref}=50$ rpm (low speed) and $\omega_{ref}=180$ rpm (high speed) have been shown in Fig. 7 and Fig. 8, respectively. These figures show effectiveness of the proposed method in extensive range of motor speed.

However, in high speeds, reactance of the stator windings is increased, so electrical time constant is increased and therefore the phase currents don't match with the flat top portion of the corresponding trapezoidal back-EMF to generate constant torque. This delay time cause to increase the torque ripple.

The motor speed control is presented such that the reference torque can be achieved by comparing motor speed with the reference speed and a PI controller block.

When reference speed increase or decrease as shown in Fig. 9, motor speed with the reference speed is compared and the reference torque achieved. So, electromagnetic torque is changed such that motor enable to tracking reference speed.

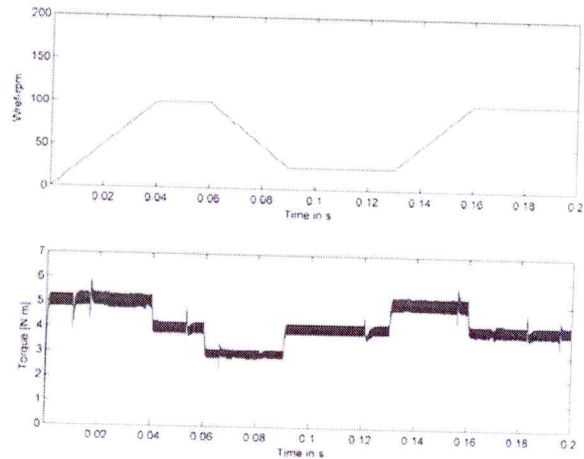


Fig. 9. Reference speed and electromagnetic torque in proposed method

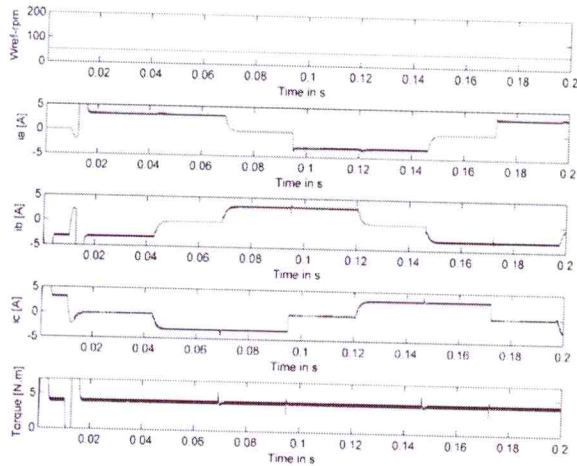


Fig. 7. Phase currents and generated torque with proposed method in $\omega_{ref}=50$ rpm (low speed)

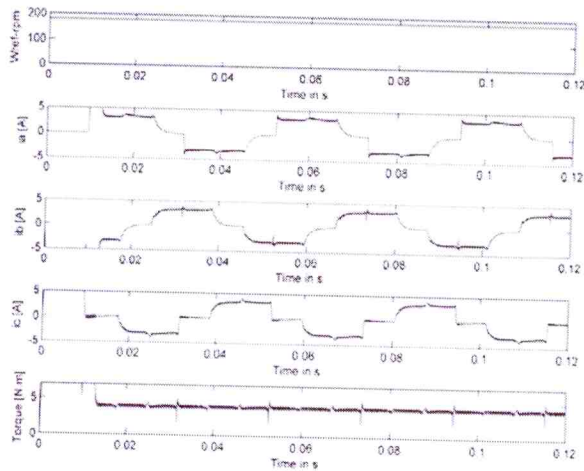


Fig. 8. Phase currents and generated torque with proposed method in $\omega_{ref}=180$ rpm (high speed)

VI. Conclusion

In this paper a novel scheme of low-cost position sensorless direct torque control of brushless DC motor drive using four-switch, three phase inverter is presented. Compared to the three-phase DTC technique, in this approach the cost reduction is achieved via reducing number of power switches and related circuits such as power supplies and drivers and simultaneously elimination of position hall effect sensors.

The proposed method decrease overall cost of BLDC drives without increasing torque and current ripple. In addition, this method is effective in extensive range of motor speed; however the torque ripple in the high speeds is more than the low speeds because of more reactance of the stator windings. The validity of the presented sensorless method is shown via simulations.

References

- [1] Gatto, G., Marongiu, I., Meo, S., Perfetto, A., Serpi, A., Predictive control of brushless DC motor drive providing minimum joule losses and torque ripple free commutation, (2011) *International Review on Modelling and Simulations (IREMOS)*, 4 (4), pp. 1500-1505.
- [2] Gatto, G., Marongiu, I., Meo, S., Perfetto, A., Serpi, A., Predictive control of brushless DC generators, (2011) *International Review of Electrical Engineering (IREE)*, 6 (5), pp. 2368-2375.
- [3] P. Pillay, R. Krishnan, Modeling, simulation, and analysis of permanent-magnet motor drives. II: The Brushless DC Motor Drive, *IEEE Trans. on Industry Applications*, vol. 25, no. 2, Mar./Apr. 1989, pp. 274-279.
- [4] J.H. Lee, S.C. Ahn, D.S. Hyun, A BLDCM drive with trapezoidal back EMF using four-switch three phase inverter, in *Proc. IEEE IAS Annu. Meet.*, vol. 3, Oct. 8-12, 2000, pp. 1705-1709.
- [5] B.K. Lee, T.K. Kim, M. Ehsani, On the feasibility of four-switch three-phase BLDC motor drives for low cost commercial applications: Topology and control, *IEEE Trans. Power. Electron.*, vol. 18, no. 1, Jan. 2003, pp. 164-172.
- [6] S.H. Park, T.S. Kim, S.C. Ahn, D.S. Hyun, A simple current control algorithm for torque ripple reduction of brushless dc motor using four-switch three-phase inverter, in *Proc. IEEE PESC Annu. Meet.*, vol. 2, Jun. 15-19, 2003, pp. 574-579.

- [7] C.T. Lin, C.W. Hung, C.W. Liu, Position sensorless control for four-switch three-phase brushless dc motor drives, *IEEE Trans. Power Electron.*, vol. 23, no. 1, Jan. 2008, pp. 438–444.
- [8] Y. Liu, Z.Q. Zhu, D. Howe, Direct torque control of brushless dc drives with reduced torque ripple, *IEEE Trans. Ind. Appl.*, vol. 41, no. 2, Mar./Apr. 2005, pp. 599–608.
- [9] S.B. Ozturk, H.A. Toliyat, Direct Torque Control of Brushless DC Motor with Nonsinusoidal Back-EMF, *Proc. IEEE IEMDC Biennial Meet., Antalya, Turkey*, May 2007, pp. 165–171.
- [10] S.B. Ozturk, W. Alexander, H.A. Toliyat, Direct Torque Control of Four-Switch Brushless DC Motor with Non-sinusoidal Back-EMF, *IEEE Trans. Power Elect.* vol. 25, No. 2, Feb. 2010, pp. 263–271.
- [11] R. Heidari, G.R.A. Markadeh, S. Abzari, M. Hosseinzadeh, An Improved Direct Torque Control for Torque Ripple Minimization of Four-Switch Brushless DC Motor with Trapezoidal Back-EMF, *The 20th Iranian Conference on Electrical Engineering (ICEE)*, May 15–17, 2012, Tehran, Iran.
- [12] A. Halvaei Niasar, A. Vahedi, H. Moghbelli, Low-cost sensorless control of four-switch, brushless DC motor drive with direct back-EMF detection, *Journal of Zhejiang University SCIENCE A*, 2009 10(2), pp. 201–208.
- [13] J.P. Johnson, M. Ehsani, Y. Guzelgunler, Review of Sensorless Methods for Brushless DC, in *Proc of the 34th IEEE IAS Annual Meeting Conference*, vol. 1, 1999, pp. 143–150.

Authors' information



Seyed Mahdi Seyedi was born in Kashan, Iran in 1982. He received his B.Sc. in 2005 from University of Kashan in electrical engineering.

He is currently M.Sc. student in the Department of Electrical Engineering, at University of Kashan. His current research interests include power electronics, advanced control of electric machines, in particular sensorless and direct

torque control of permanent magnet synchronous and brushless dc motors.



Abolfazl Halvaei Niasar was born in Kashan, Iran in 1974. He received his B.Sc., M.Sc., and Ph.D. in 1998, 2000, and 2008 from Isfahan University of Technology (IUT), university of Tehran (UT) and Iran University of Science and Technology (IUST) all in electrical engineering respectively.

He is currently with the Faculty of Electrical and Computer Engineering, at University of Kashan, Iran. His research interests are mainly PM and Brushless DC motor drives, sensorless drives, DSP based control systems and the industrial control systems. Dr. Halvaei is a member of the Institute of Electrical and Electronics Engineers (IEEE).



Hassan Moghbelli was born in Isfahan, Iran in 1950. He received his B.S., M.S. and Ph.D. in 1973, 1978 and 1989 from Iran University of Science and Technology (IUST), Oklahoma State University and University of Missouri-Columbia (UMC) all in electrical engineering respectively. He has directed several projects in the area of electric drives, power systems,

electric vehicles, hybrid electric and fuel cell vehicles and railway electrification. His research interests are electric drives, power electronics, and design of electric and hybrid electric vehicle. He is a member of IEEE, ASME, and SAE